

VHE Gamma-Ray Induced Pair Cascades in the Radiation Fields of Dust Tori of AGN: Application to Cen A

P. Roustazadeh and M. Böttcher¹

ABSTRACT

The growing number of extragalactic high-energy (HE, $E > 100$ MeV) and very-high-energy (VHE, $E > 100$ GeV) γ -ray sources that do not belong to the blazar class suggests that VHE γ -ray production may be a common property of most radio-loud Active Galactic Nuclei (AGN). In a previous paper, we have investigated the signatures of Compton-supported pair cascades initiated by VHE γ -ray absorption in monochromatic radiation fields, dominated by Ly α line emission from the Broad Line Region. In this paper, we investigate the interaction of nuclear VHE γ -rays with the thermal infrared radiation field from a circumnuclear dust torus. Our code follows the spatial development of the cascade in full 3-dimensional geometry. We provide a model fit to the broadband SED of the dust-rich, γ -ray loud radio galaxy Cen A and show that typical blazar-like jet parameters may be used to model the broadband SED, if one allows for an additional cascade contribution to the *Fermi* γ -ray emission.

Subject headings: galaxies: active — galaxies: jets — gamma-rays: galaxies — radiation mechanisms: non-thermal — relativistic processes

1. Introduction

Blazars are a class of radio-loud active galactic nuclei (AGNs) comprised of Flat-Spectrum Radio Quasars (FSRQs) and BL Lac objects. Their spectral energy distributions (SEDs) are characterized by non-thermal continuum spectra with a broad low-frequency component in the radio – UV or X-ray frequency range and a high-frequency component

¹Astrophysical Institute, Department of Physics and Astronomy, Ohio University, Athens, OH 45701, USA

from X-rays to γ -rays, and they often exhibit substantial variability across the electromagnetic spectrum. In the VHE γ -ray regime, the time scale of this variability has been observed to be as short as just a few minutes (Albert et al. 2007; Aharonian et al. 2007). While previous generations of ground-based Atmospheric Cherenkov Telescope (ACT) facilities detected almost exclusively high-frequency peaked BL Lac objects (HBLs) as extragalactic sources of VHE γ -rays (with the notable exception of the radio galaxy M87), in recent years, a number of non-HBL blazars and even non-blazar radio-loud AGN have been detected by the current generation of ACTs. This suggests that most blazars might be intrinsically emitters of VHE γ -rays. According to AGN unification schemes (Urry & Padovani 1995), radio galaxies are the mis-aligned parent population of blazars with the less powerful FR I radio galaxies corresponding to BL Lac objects and FR II radio galaxies being the parent population of radio-loud quasars. Blazars are those objects which are viewed at a small angle with respect to the jet axis. If this unification scheme holds, then, by inference, also radio galaxies may be expected to be intrinsically emitters of VHE γ -rays within a narrow cone around the jet axis.

While there is little evidence for dense radiation environments in the nuclear regions of BL Lac objects — in particular, HBLs —, strong line emission in Flat Spectrum Radio Quasars (FSRQs) as well as the occasional detection of emission lines in the spectra of some BL Lac objects (e.g., Vermeulen et al. 1995) indicates dense nuclear radiation fields in those objects. This is supported by spectral modeling of the SEDs of blazars using leptonic models which prefer scenarios based on external radiation fields as sources for Compton scattering to produce the high-energy radiation in FSRQs, LBLs and also some IBLs (e.g., Ghisellini et al. 1998; Madejski et al. 1999; Böttcher & Bloom 2000; Acciari et al. 2008). If the VHE γ -ray emission is indeed produced in the high-radiation-density environment of the broad line region (BLR) and/or the dust torus of an AGN, it is expected to be strongly attenuated by $\gamma\gamma$ pair production (e.g. Protheroe & Biermann 1997; Donea & Protheroe 2003; Reimer 2007; Liu et al. 2008; Sitarek & Bednarek 2008). Aharonian et al. (2008) have suggested that such intrinsic $\gamma\gamma$ absorption may be responsible for producing the unexpectedly hard intrinsic (i.e., after correction for $\gamma\gamma$ absorption by the extragalactic background light) VHE γ -ray spectra of some blazars at relatively high redshift. A similar effect has been invoked by Poutanen & Stern (2010) to explain the spectral breaks in the *Fermi* spectra of γ -ray blazars. This absorption process will lead to the development of Compton-supported pair cascades in the circumnuclear environment (e.g., Bednarek & Kirk 1995; Sitarek & Bednarek 2010; Roustazadeh & Böttcher 2010).

In Roustazadeh & Böttcher (2010), we considered the full 3-dimensional development of a Compton-supported VHE γ -ray induced cascade in a monochromatic radiation field. This was considered as an approximation to BLR emission dominated by a single (e.g.,

$\text{Ly}\alpha$) emission line. In that work, we showed that for typical radio-loud AGN parameters rather small ($\sim \mu\text{G}$) magnetic fields in the central ~ 1 pc of the AGN may lead to efficient isotropization of the cascade emission in the *Fermi* energy range. We applied this idea to fit the *Fermi* γ -ray emission of the radio galaxy NGC 1275 (Abdo et al. 2009a) under the plausible assumption that this radio galaxy would appear as a γ -ray bright blazar when viewed along the jet axis.

In this paper, we present a generalization of the Monte-Carlo cascade code developed in Roustazadeh & Böttcher (2010) to arbitrary radiation fields. In particular, we will focus on thermal blackbody radiation fields, representative of the emission from a circum-nuclear dust torus. In Section 2 we will outline the general model setup and assumptions and describe the modified Monte-Carlo code that treats the full three-dimensional cascade development. Numerical results for generic parameters will be presented in Section 3. In Section 4, we will demonstrate that the broad-band SED of the radio galaxy Cen A, including the recent *Fermi* γ -ray data (Abdo et al. 2009c), can be modeled with plausible parameters expected for a mis-aligned blazar, allowing for a contribution from VHE γ -ray induced cascades in the *Fermi* energy range. We summarize in Section 5.

2. Model Setup and Code Description

Figure 1 illustrates the geometrical setup of our model system. We represent the primary VHE γ -ray emission as a mono-directional beam of γ -rays propagating along the X axis, described by a power-law with photon spectrum index α and a high-energy cut-off at $E_{\gamma,max}$. For the following study, we assume that the primary γ -rays interact via $\gamma\gamma$ absorption and pair production with an isotropic thermal blackbody radiation field within a fixed boundary, given by a radius R_{ext} , i.e.,

$$u_{ext}(\nu, r, \Omega) = 2h\nu^3/c^3 \frac{A}{\exp(\frac{h\nu}{kT}) - 1} H(R_{ext} - r) \quad (1)$$

where A is a normalization factor chosen to obtain a total radiation energy density u_{ext} (see Eq. 2 below), and H is the Heaviside function, $H(x) = 1$ if $x > 0$ and $H(x) = 0$ otherwise. A magnetic field of order $\sim \text{mG}$ is present. Without loss of generality, we choose the y and z axes of our coordinate system such that the magnetic field lies in the (x,y) plane.

The input parameters to our model simulation describing the external radiation field are the integral of $u_{ext}(\nu, r, \Omega)$ over all frequencies:

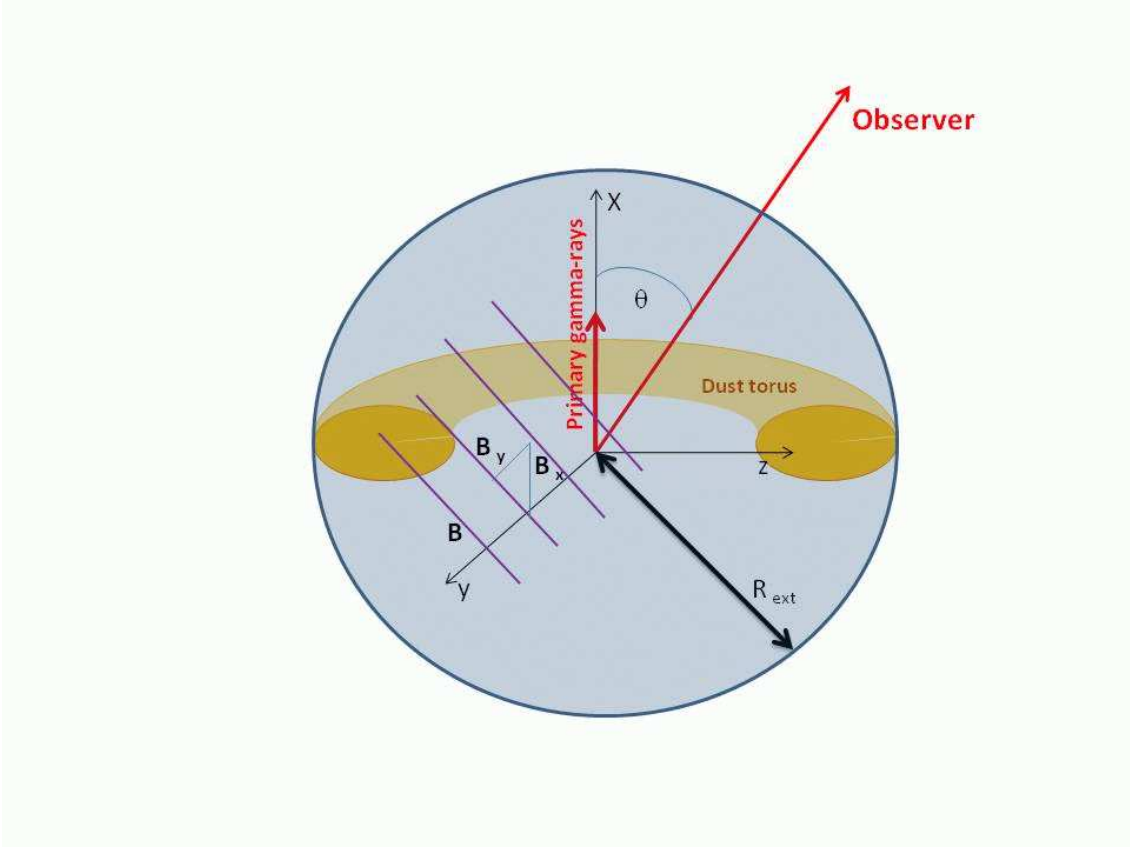


Fig. 1.— Geometry of the model setup.

$$u_{\text{ext}} = 4\pi \int_0^\infty u_{\text{ext}}(\nu, r, \Omega) d\nu, \quad (2)$$

the blackbody temperature T , and the radial extent R_{ext} .

We have used the Monte-Carlo code developed by Roustazadeh & Böttcher (2010). This code evaluates $\gamma\gamma$ absorption and pair production using the full analytical solution to the pair production spectrum of Böttcher & Schlickeiser (1997) under the assumption that the produced electron and positron travel along the direction of propagation of the incoming γ -ray. The trajectories of the particles are followed in full 3-D geometry. Compton scattering is evaluated using the head-on approximation, assuming that the scattered photon travels along the direction of motion of the electron/positron at the time of scattering. While the Compton energy loss to the electron is properly accounted for, we neglect the recoil effect on the travel direction of the electron. In order to improve the statistics of the otherwise very few highest-energy photons, we introduce a statistical weight, w , inversely proportional to the square of the photon energy, $w = 1/\epsilon^2$. Where $\epsilon = \frac{E_\gamma}{m_e c^2}$.

To save CPU time, we precalculate tables for the absorption opacity $\kappa_{\gamma\gamma}$, Compton scattering length λ_{IC} , and Compton cross section for each photon energy, electron energy and interaction angle before the start of the actual simulation.

The simulation produces a photon event file, logging the energy, statistical weight, and travel direction of every photon that escapes the region bounded by R_{ext} . A separate post-processing routine is then used to extract angle-dependent photon spectra with arbitrary angular and energy binning from the log files.

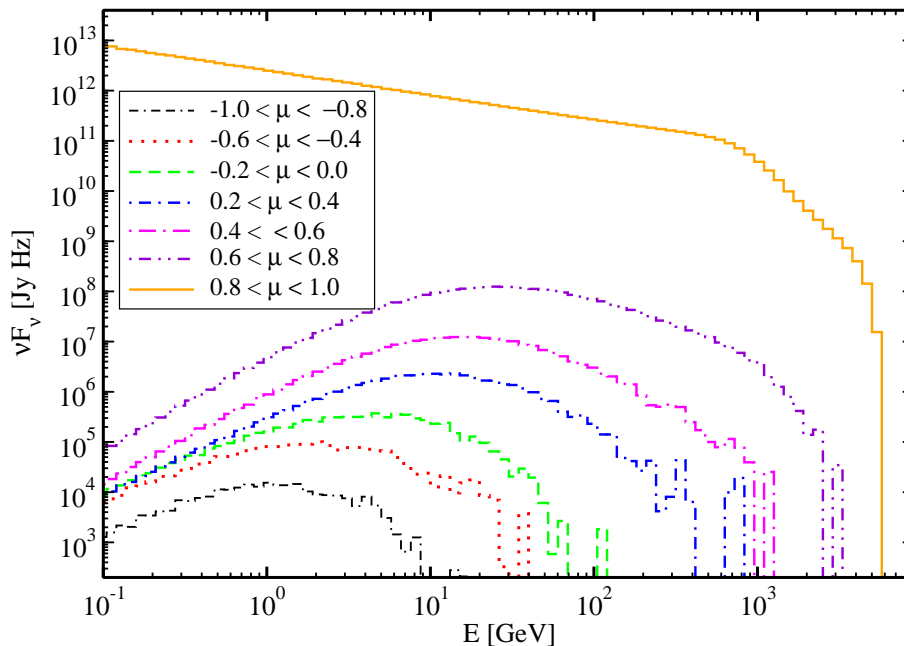


Fig. 2.— Cascade emission at different viewing angles ($\mu = \cos \theta_{\text{obs}}$). Parameters: $B = 1$ mG, $\theta_B = 5^\circ$; $u_{\text{ext}} = 10^{-5}$ erg cm $^{-3}$, $R_{\text{ext}} = 10^{18}$ cm, $T = 1000$ K, $\alpha = 2.5$, $E_{\gamma,\text{max}} = 5$ TeV.

3. Numerical Results

For comparison with our previous study on mono-energetic radiation fields, we conduct a similar parameter study as presented in (Roustazadeh & Böttcher 2010), investigating the effects of parameter variations on the resulting angle-dependent photon spectra. Standard parameters for most simulations in our parameter study are: a magnetic field of $B = 1$ mG, oriented at an angle of $\theta_B = 5^\circ$ with respect to the X axis ($B_x = 1$ mG, $B_y = 0.1$ mG); an

external radiation energy density of $u_{\text{ext}} = 10^{-5} \text{ erg cm}^{-3}$, extended over a region of radius $R_{\text{ext}} = 10^{18} \text{ cm}$; a blackbody temperature of $T = 10^3 \text{ K}$ (corresponding to a peak of the blackbody spectrum at a photon energy of $E_s^{\text{pk}} = 0.25 \text{ eV}$). The incident γ -ray spectrum has a photon index of $\alpha = 2.5$ and extends out to $E_{\gamma, \text{max}} = 5 \text{ TeV}$. The emanating photon spectra for all directions have been normalized with the same normalization factor, corresponding to a characteristic flux level of a γ -ray bright (*Fermi*) blazar in the forward direction.

Figure 2 illustrates the viewing angle dependence of the cascade emission. The $\gamma\gamma$ absorption cut-off at an energy $E_c = (m_e c^2)^2 / E_s \sim 1 \text{ TeV}$ is very smooth in this simulation because of the broad thermal blackbody spectrum of the external radiation field. In contrast, the δ -function approximation for the external radiation field adopted in Roustazadeh & Böttcher (2010) resulted in an artificially sharp cutoff in that work.

At off-axis viewing angles, the observed spectrum is exclusively the result of the cascade. In the limit of low photon energies (far below the $\gamma\gamma$ absorption threshold) and neglecting particle escape from the cascade zone, one expects a low-frequency shape close to $\nu F_\nu \propto \nu^{1/2}$ due to efficient radiative cooling of secondary particles injected at high energies (Roustazadeh & Böttcher 2010). However, with the typical parameters used for this parameter study, the assumption of negligible particle escape is not always justified. In order to estimate the possible suppression of the low-frequency cascade emission due to particle escape, we calculate the critical electron energy for which the Compton cooling time scale $\tau_{\text{IC}}(\gamma)$ equals the escape time scale, $\tau_{\text{esc}} = R_{\text{ext}} / (c \cos \theta_B)$. Using a characteristic thermal photon energy of $\epsilon_{\text{Th}} = 2.8 kT / (m_e c^2)$, the resulting Compton scattered photon energy, ϵ_{esc} below which we expect to see the effects of particle escape and, hence, inefficient radiative cooling, is

$$\epsilon_{\text{esc}} = \frac{9 \times 2.8 kT m_e c^2 \cos^2 \theta_B}{16 \sigma_T^2 u_{\text{ext}}^2 R_{\text{ext}}^2} \quad (3)$$

corresponding to an actual energy (in GeV) of

$$E_{\text{esc}} \approx 2 T_3 u_{-5}^{-2} R_{18}^{-2} \cos^2 \theta_B \text{ GeV} \quad (4)$$

where $T = 10^3 T_3 \text{ K}$, $u_{\text{ext}} = 10^{-5} u_{-5} \text{ erg cm}^{-3}$, and $R = 10^{18} R_{18} \text{ cm}$. Therefore, for our standard parameters, we expect the low-frequency ($E \lesssim$ a few GeV) to be significantly affected by particle escape. This explains why the low-energy photon spectra shown in Figure 2 are harder than $\nu^{1/2}$. The cascade emission is progressively suppressed at high energies with increasing viewing angle due to incomplete isotropization of the highest-energy secondary particles. This effect becomes important beyond the energy $E_{\text{IC,br}}$ of Compton-scattered photons by secondary electrons/positrons for which the Compton-scattering length

λ_{IC} equals the distance travelled along the gyration motion over an angle θ , $\lambda_{IC}(\gamma) = \theta r_{\text{gyr}}(\gamma)$, which is given by

$$E_{IC,br} = \frac{3 e B}{4 \sigma_T u_{\text{ext}} \theta} E_s \sim 1.3 B_{-3} u_{-5}^{-1} T_3 \theta^{-1} \text{ GeV}. \quad (5)$$

where $B = 10^{-3}$ mG (Roustazadeh & Böttcher 2010).

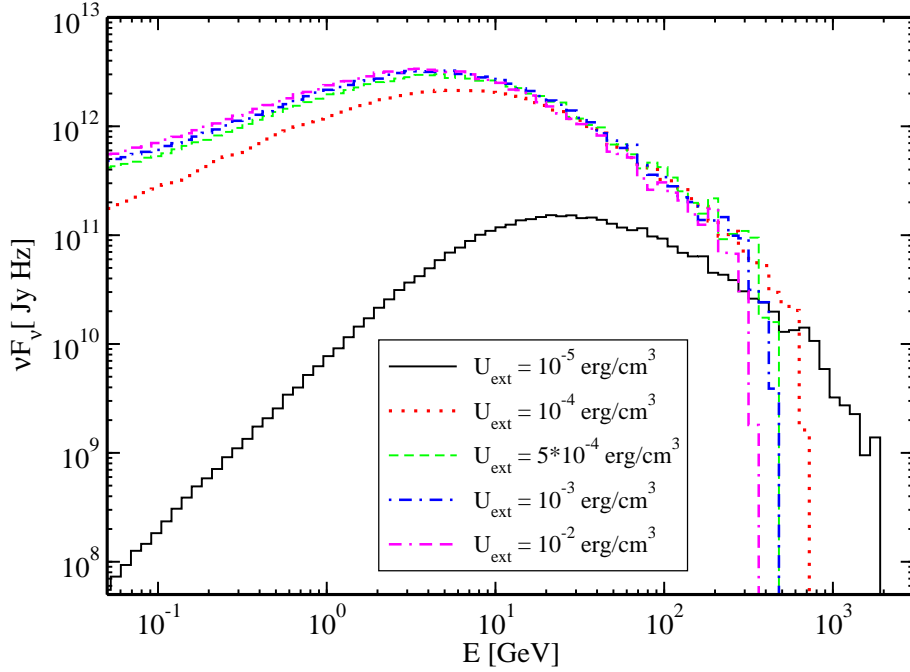


Fig. 3.— The effect of a varying external radiation energy density. Parameters: $B_x = 10^{-3}$ G, $B_y = 1.3 \times 10^{-4}$ G, $\theta_B = 7.4^\circ$; and other parameters are the same as for Figure 2 in the angular bin $0.4 \leq \mu \leq 0.6$

Figure 3 shows the cascade spectra for different values of the external radiation field energy density u_{ext} . For large energy densities $u_{\text{ext}} \gtrsim 10^{-4}$ erg cm $^{-3}$, $\tau_{\gamma\gamma} \gg 1$ for photons above the pair production threshold $\gamma\gamma$ so that essentially all VHE photons will be absorbed and the photon flux from the cascade becomes independent of u_{ext} .

The figure confirms our discussion concerning escape and hence inefficient radiative cooling of low-energy particles above (see Eq. 4). For large values of u_{ext} , the Compton loss time scale for all relativistic electrons producing γ -rays in the considered range, is much

shorter than the escape time scale. Hence, the expected $\nu F_\nu \propto \nu^{1/2}$ shape results. In the low- u_{ext} case, escape affects even ultrarelativistic electrons, resulting in a substantial hardening of the low-energy photon spectrum.

Figure 4 illustrates the effect of a varying temperature of the external blackbody radiation field. As the temperature increases up to 1000 K the cascade flux increases because the $\gamma\gamma$ absorption threshold energy decreases so that an increasing fraction of γ -rays can be absorbed. The isotropization turnover is almost independent of T . For temperatures $T > 1000$ K the cascade flux decreases with increasing T because u_{ext} remains fixed, leading to a decreasing photon number density and absorption opacity $\kappa_{\gamma\gamma}$ with increasing T (and, hence, increasing E_s). The figure also confirms our expectation (Eq. 4) that an increasing blackbody temperature leads to an increasing suppression of the low-frequency portion of the cascade emission due to particle escape.

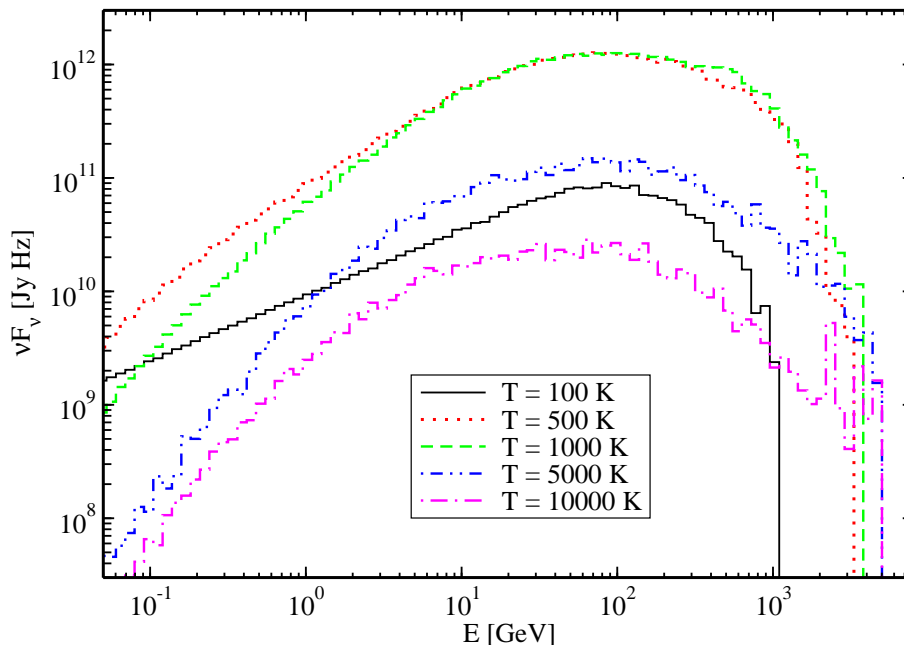


Fig. 4.— The effect of a varying temperature of the external blackbody radiation field. $\theta_B = 15^\circ$ and other parameters are the same as for Figure 2 in the angular bin $0.4 \leq \mu \leq 0.6$

Figures 5 and 6 illustrate the effects of varying magnetic-field parameters (strength and orientation). As expected, the results are essentially the same as for cascades in monoenergetic radiation fields investigated in Roustazadeh & Böttcher (2010): The cascade

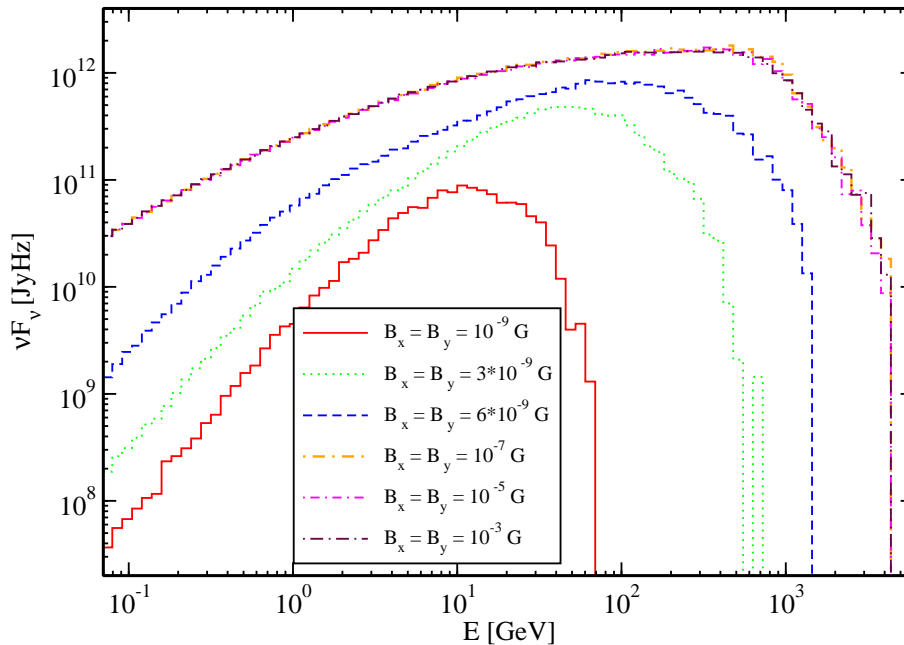


Fig. 5.— The effect of a varying magnetic field strength, for a fixed angle of $\theta_B = 45^\circ$ between jet axis and magnetic field. All other parameters are the same as for Figure 2 in the angular bin $0.4 \leq \mu \leq 0.6$

development is extremely sensitive to the transverse magnetic field B_y . The limit in which even the highest-energy secondary particles are effectively isotropized before undergoing the first Compton scattering interaction, is easily reached for typical magnetic fields expected in the circum-nuclear environment of AGNs.

4. Application to Cen A

The standard AGN unification scheme (Urry & Padovani 1995) proposes that blazars and radio galaxies are intrinsically identical objects viewed at different angles with respect to the jet axis. According to this scheme, FR I and FR II radio galaxies are believed to be the parent population of BL Lac objects and FSRQs, respectively. Hence, if most blazars, including LBLs and FSRQs, are intrinsically VHE γ -ray emitters potentially producing pair cascades in their immediate environments, the radiative signatures of these cascades might be observable in many radio galaxies. In fact, *EGRET* provided evidence for > 100 MeV γ -ray

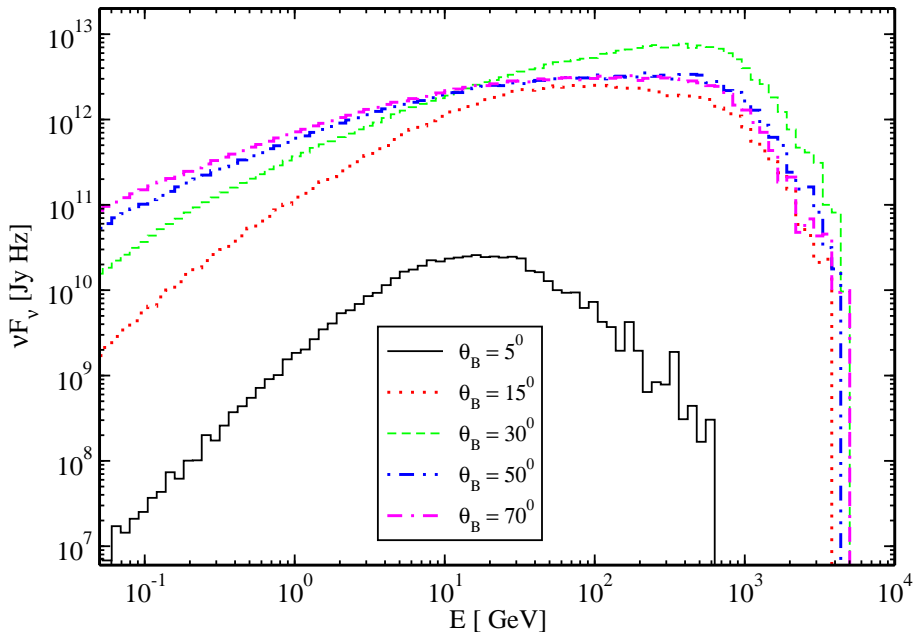


Fig. 6.— The effect of a varying magnetic field orientation, for a fixed magnetic field strength of $B = 1$ mG. All other parameters are the same as for Figure 2 in the angular bin $0.4 \leq \mu \leq 0.6$

emission from three radio galaxies (Cen A: Sreekumar et al. (1999), 3C 111: Hartman et al. (2008), and NGC 6251: Mukherjee et al. (2002)). These sources have been confirmed as high-energy γ -ray sources by *Fermi* (Abdo et al. 2009c, 2010b), along with the detection of five more radio galaxies (NGC 1275: Abdo et al. (2009a), M 87: Abdo et al. (2009b), 3C 120, 3C 207, and 3C 380: Abdo et al. (2010b)). In this paper, we focus on the radio galaxy Cen A (Abdo et al. 2009c).

The FR I Cen A is the nearest radio-loud active galaxy to Earth. It has a redshift of $z=0.00183$ at the distance of $D = 3.7$ Mpc. Recently, the Auger collaboration reported that the arrival directions of the highest energy cosmic rays ($E \gtrsim 6 \times 10^{19}$ eV) observed by the Auger observatory are correlated with nearby AGN, including Cen A (Abraham, J., et al. 2007, 2008). This suggests that Cen A may be the dominant source of observed UHECR nuclei above the GZK cut off.

Cen A has an interesting radio structure on several size scales. The most prominent features are its giant radio lobes, which subtend $\sim 10^0$ on the sky, oriented primarily in

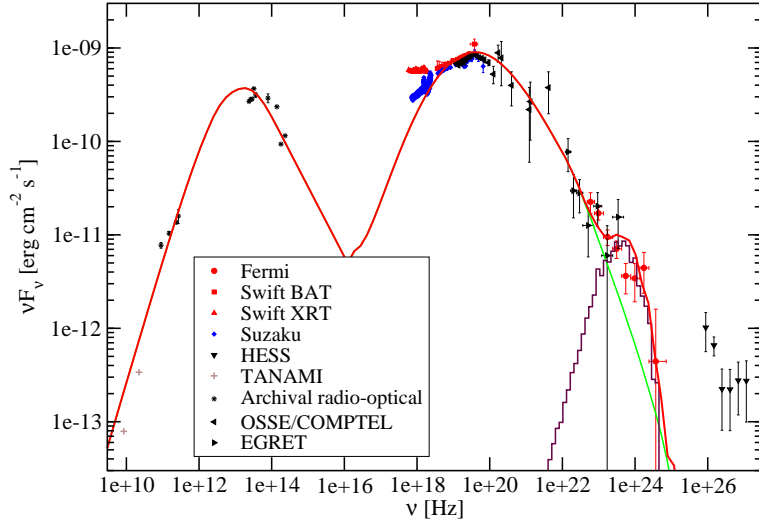


Fig. 7.— Fit to the SED of Cen A. The green curve is a fit to the broad-band SED using the model of (Böttcher & Chiang 2002), while the maroon curve is the cascade emission resulting from $\gamma\gamma$ absorption of the forward jet emission. The red curve is the sum of both contributions (viewed at an angle of 70°).

the north-south direction. They have been imaged at 4.8 GHz by the Parkes telescope (Junkes et al. 1993) and studied at up to ~ 60 GHz by Hardcastle et al. (2009). The radio lobes are the only extragalactic source structure that has so far been spatially resolved in GeV γ -rays by *Fermi* (Abdo et al. 2010c). The innermost region of Cen A has been resolved with VLBI and shown to have a size of $\sim 3 \times 10^{16}$ cm (Kellermann et al. 1997; Horiuchi et al. 2006). Observations at shorter wavelengths also reveal a small core. VLT infrared interferometry resolves the core size to $\sim 6 \times 10^{17}$ cm (Meisenheimer et al. 2007). The angle of the sub-parsec jet of Cen A to our line of sight is $\sim 50^\circ - 80^\circ$ (Tingay et al. 1998) with a preferred value of $\sim 70^\circ$ (Steinle 2009).

The K-band nuclear flux with starlight subtracted is $F(K) \sim 38$ mJy, corresponding to $\nu L_\nu \sim 7 \times 10^{40}$ erg s^{-1} for a distance of 3.5 Mpc (Marconi et al. 2000). The mid-IR flux of ~ 1.6 Jy at $11.7 \mu\text{m}$ corresponds to $\nu L_\nu \sim 6 \times 10^{41}$ erg s^{-1} . The broadband SED from radio to γ -rays has been fitted with a synchrotron self-Compton model by Abdo et al. (2010a). In their model (see Table 2 of Abdo et al. 2010a), a maximum electron Lorentz factor of $\gamma_{max} = 1 \times 10^8$ was required in order to produce the observed γ -ray emission. However, given the assumed magnetic field of $B = 6.2$ G, this does not seem possible since for $\gamma = 10^8$ electrons, the synchrotron loss time scale is shorter than their gyro-timescale, which sets the shortest plausible acceleration time scale. Here, we therefore present an alternative interpretation of the SED, based on the plausible assumption that Cen A would appear as a

VHE γ -ray emitting blazar in the jet direction, and cascading of VHE γ -rays on the nuclear infrared radiation field produces an observable off-axis γ -ray signature in the *Fermi* energy range.

Figure 7 illustrates a broadband fit to the SED of Cen A (data from Abdo et al. 2010a), using the equilibrium version of the blazar radiation transfer code of Böttcher & Chiang (2002), as described in more detail in Acciari et al. (2009). For this fit, standard blazar jet parameters were adopted, but the viewing angle was chosen in accord with the observationally inferred range. Specifically, we chose $\theta_{\text{obs}} = 70^\circ$. Other model parameters include a bulk Lorentz factor of $\Gamma = 5$, a radius of the emission region of $R = 1 \times 10^{16}$ cm, a kinetic luminosity in relativistic electrons, $L_e = 9.4 \times 10^{43}$ erg s $^{-1}$, a co-moving magnetic field of $B = 11$ G, corresponding to a luminosity in the magnetic field (Poynting flux) of $L_B = 1.1 \times 10^{45}$ erg s $^{-1}$ and a magnetic-field equipartition fraction $\epsilon_B \equiv L_B/L_e = 12$, corresponding to a Poynting-flux dominated jet. Electrons are injected into the emission region at a steady rate, with a distribution characterized by low- and high-energy cutoffs at $\gamma_1 = 1.2 \times 10^3$ and $\gamma_2 = 1.0 \times 10^6$, respectively, and a spectral index of $q = 3.5$. The code finds a self-consistent equilibrium between particle injection, radiative cooling and escape, from which the final photon spectrum is calculated. The resulting broadband SED fit is illustrated by the solid green curve in Figure 7. The flux emanating in the forward direction ($\theta_{\text{obs}} = 0^\circ$, i.e., the blazar direction) has been chosen as an input to our cascade simulation to evaluate the cascade emission in the nuclear infrared radiation field of Cen A observed at the given angle of $\theta_{\text{obs}} = 70^\circ$.

For the cascade simulation, we assumed a blackbody temperature of 2300 K resulting in a peak frequency in the K-band. The external radiation field is parameterized through $u_{\text{ext}} = 1.5 \times 10^{-3}$ erg cm $^{-3}$ and $R_{\text{ext}} = 3 \times 10^{16}$ cm. These parameters combine to an IR luminosity of $L_{\text{BLR}} = 4\pi R_{\text{ext}}^2 c u_{\text{ext}} = 5 \times 10^{41}$ erg s $^{-1}$, in agreement with mid-IR flux observed for Cen A (Marconi et al. 2000). The magnetic field is $B = 1$ mG, oriented at an angle of $\theta_B = 4^\circ$. The cascade spectrum shown in Figure 7 pertains to the angular bin $0.28 < \mu < 0.38$ (corresponding to $67^\circ \lesssim \theta \lesssim 73^\circ$), appropriate for the known orientation of Cen A and consistent with our broadband SED fit parameters. The cascade spectrum is shown by the maroon curve in Figure 7, while the total observed spectrum is the solid red curve. The figure illustrates that the cascade contribution in the *Fermi* range substantially improves the fit, while still allowing physically reasonable parameters for the broadband SED fit.

5. Summary

We investigated the signatures of Compton-supported pair cascades initiated by the interaction of nuclear VHE γ -rays with the thermal infrared radiation field of a circumnuclear dust torus in AGNs. We follow the spatial development of the cascade in full 3-dimensional geometry and study the dependence of the radiative output on various parameters pertaining to the infrared radiation field and the magnetic field in the cascade region.

We confirm the results of our previous study of cascades in monoenergetic radiation fields that small ($\gtrsim \mu\text{G}$) perpendicular (to the primary VHE γ -ray beam) magnetic field components lead to efficient isotropization of the cascade emission out to HE γ -ray energies. The cascade intensity as well as the location of a high-energy turnover due to inefficient isotropization also depend sensitively on the energy density and temperature of the soft blackbody radiation field, as long as the cascade is not saturated in the sense that not all VHE γ -rays are absorbed.

The shape of the low-frequency tail of the cascade emission is a result of the interplay between radiative cooling and escape. For environments characterized by efficient radiative cooling, the canonical $\nu F_\nu \propto \nu^{1/2}$ spectrum results. If radiative cooling is inefficient compared to escape, the low-frequency cascade spectra are harder than $\nu^{1/2}$.

We provide a model fit to the broadband SED of the dust-rich, γ -ray loud radio galaxy Cen A. We show that typical blazar-like jet parameters may be used to model the broadband SED, if one allows for an additional cascade contribution to the *Fermi* γ -ray emission due to $\gamma\gamma$ absorption and cascading in the thermal infrared radiation field of the prominent dust emission known to be present in Cen A.

We thank J. Finke for providing the SED data points of Cen A. This work was supported by NASA through Fermi Guest Investigator Grants NNX09AT81G and NNX10AO49G.

REFERENCES

- Abdo, A. A., et al., 2009a, ApJ, 699, 31
 Abdo, A. A., et al., 2009b, ApJ, 707, 55
 Abdo, A. A., et al., 2009c, ApJ, 700, 597
 Abdo, A. A., et al., 2010a, ApJ, 719, 1433

- Abdo, A. A., et al., 2010b, *ApJ*, 720, 912
- Abdo, A. A., et al., 2010c, *Science*, 328, 725
- Abraham, J., et al., 2007, *Science*, 318, 938
- Abraham, J., et al., 2008, *Astropar. Phys.*, 29, 188
- Acciari, V. A., et al., 2008, *ApJ*, 684, L73
- Acciari, V. A., et al., 2009, *ApJ*, 707, 612
- Aharonian, F., et al., 2007, *ApJ*, 664, L71
- Aharonian, F. A., Khangulyan, D., & Costamante, L., 2008, *MNRAS*, 387, 1206
- Albert, J., et al., 2007, *ApJ*, 669, 862
- Bednarek, W., & Kirk, J. G., 1995, *A&A*, 294, 366
- Böttcher, M., & Chiang, J., 2002, *ApJ*, 581, 127
- Böttcher, M., & Bloom, S. D., 2000, *AJ*, 119, 469
- Böttcher, M., & Schlickeiser, R., 1997, *A&A*, 325, 866
- Böttcher, M., 2007, in proc. “The Multimessenger Approach to Gamma-Ray Sources”, *ApSS*, 309, 95
- Dermer, C. D., & Böttcher, M., 2006, *ApJ*, 643, 1081
- Donea, A. C., & Protheroe, R. J., 2003, *Astrop. Phys.*, 18, 337
- Ghisellini, G., et al., 1998, *MNRAS*, 301, 451
- Hartman, R. C., Kadler, M., & Tueller, J., 2008, *ApJ*, 688, 852
- Hardcastle, M. J., Cheung, C. C., Feain, I. J., & Stawarz, L., 2009, *MNRAS*, 393, 1041
- Horiuchi, S., Meier, D. L., Preston, R. A., & Tingay, S. J., 2006, *PASJ*, 58, 211
- Junkes, N., Haynes, R. F., Harnett, J. I., & Jauncy, D. L., 1993, *A&A*, 269, 29
- Kellerman, K. I., Zensus, J. A., & Cohen, M. H., 1997, *ApJ*, 475, L93
- Liu, H. T., Bai, J. M., & Ma, L., 2008, *ApJ*, 688, 148

- Madejski, G. M., et al., 1999, *ApJ*, 521, 145
- Marconi, A., Schreire, E. J., Koekemoer, A., Capetti, A., Axon, D., Maccetto, D., & Caon, N. 2000, *ApJ*, 528, 276
- Meisenheimer, K., et al., 2007, *A& A*, 471, 453
- Mukherjee, R., Halpern, J., Mirabal, N., & Gotthelf, E. V., 2002, *ApJ*, 574, 693
- Poutanen, J., & Stern, B., 2010, *ApJ*, 717, L118
- Protheroe, R. J., 1986, *MNRAS*, 221, 769
- Protheroe, R. J., & Biermann, P. L., 1997, *Astrop. Phys.*, 6, 293
- Reimer, A., 2007, *ApJ*, 665, 1023
- Roustazadeh, P., & Böttcher, M., 2010, *ApJ*, 717, 468
- Sitarek, J., & Bednarek, W., 2008, *MNRAS*, 391, 624
- Sitarek, J., & Bednarek, W., 2010, *MNRAS*, 401, 1983
- Sreekumar, P., Bertsch, D. L., Hartman, R. C., Nolan, P. L., & Thompson, D. J., 1999, *Astropart. Phys.*, 11, 221
- Steinle, H., 2009, in proc. of “The Many Faces of Centaurus A”, PASA, in press
- Tingay, S. J., et al., 1998, *AJ*, 115, 960
- Urry, C. M., & Padovani, P., 1995, *PASP*, 107, 803
- Vermeulen, R. C., et al., 1995, *ApJ*, 452, L5
- Zdziarski, A. A., 1988, *ApJ*, 335, 786